geosciences

MDPI

Article

# Determination of Peak Impact Force for Buildings Exposed to Structural Pounding during Earthquakes

**Seyed Mohammad Khatami [1], Hosein Naderpour [2], Rui Carneiro Barros [3], Anna Jakubczyk-Gałczyńska [4] and Robert Jankowski [4,*]**

1 Center of Semnan Municipality, University of Applied Science and Technology, Semnan 35149, Iran; m61.khatami@gmail.com
2 Faculty of Civil Engineering, Semnan University, Semnan 3513119111, Iran; naderpour@semnan.ac.ir
3 Faculty of Engineering, University of Porto (FEUP), 4200-465 Porto, Portugal; rcb@fe.up.pt
4 Faculty of Civil and Environmental Engineering, Gdansk University of Technology, 80-233 Gdansk, Poland; annjakub@pg.edu.pl
* Correspondence: jankowr@pg.edu.pl

Received: 23 November 2019; Accepted: 27 December 2019; Published: 30 December 2019


**Abstract:** Structural pounding between adjacent, insufficiently separated buildings, or bridge segments, has been repeatedly observed during seismic excitations. Such earthquake-induced collisions may cause severe structural damage or even lead to the collapse of colliding structures. The aim of the present paper was to show the results of the study focused on determination of peak impact forces during collisions between buildings exposed to different seismic excitations. A set of different ground motion records, with various peak ground acceleration (PGA) values and frequency contents, were considered. First, pounding-involved numerical analysis was conducted for the basic parameters of colliding buildings. Then, the parametric study was carried out for different structural natural periods, structural damping ratios, gap sizes between buildings and coefficients of restitution. The results of the analysis conducted for the basic structural parameters indicate that the largest response of the analysed buildings was observed for the Duzce earthquake. The parametric study showed that the pounding-involved structural response depended substantially on all parameters considered in the analysis, and the largest response was observed for different ground motions. The results of the study presented in this paper indicate that the value of the peak impact force expected during the time of the earthquake does not depend on the PGA value of ground motion, but rather on the frequency contents of excitation and pounding scenario. It is therefore recommended that the peak impact force for buildings exposed to structural pounding during earthquakes should be determined individually for the specific structural configuration taking into account the design ground motion.

**Keywords:** earthquakes; impact force; structural pounding; buildings; parametric study

## 1. Introduction

During seismic excitations, adjacent insufficiently separated buildings, or bridge segments, may collide with each other because of different dynamic characteristics or spatial seismic effects related to propagation of seismic wave [1–4]. The phenomenon, known as the earthquake-induced structural pounding, may cause severe structural damage or even lead to the collapse of colliding structures [5,6].

The effects of structural pounding during earthquakes have been intensively studied for more than three decades. Anagnostopoulos [1,7] was among the first researchers who described the philosophy of building pounding by experimental and numerical investigations. He also suggested using the linear viscoelastic model of collisions in numerical analyses. He justified the model based on coefficient

of restitution so as to be able to calculate the impact force and dissipated energy during collision. However, there is a drawback of the model, which is related to the fact that the negative impact force is observed at the end of contact which does not have any physical explanation. Later on, Jankowski [8,9] extended the formula and proposed the nonlinear viscoelastic model. The approach allows the relation between force and deformation to be determined more precisely and eliminates the drawback of the linear viscoelastic model. The Hertzdamp model was considered by Muthukumar and DesRoches [10] and by Ye et al. [11] in a modified form to simulate impact force during contact even more accurately. They showed in their studies that the impact damping ratio depends directly on impact velocity and on stiffness of impact spring which is applied in the impact force model. Moreover, Filiatrault et al. [12] presented results of shake table tests of pounding between adjacent single-bay steel framed model structures and compared them with the numerical results obtained by using two existing computer programs. Similar results were obtained from the experiments and numerical analyses, confirming the accuracy of the numerical approach considered in the study. Pounding between base-isolated structures were investigated by Komodromos et al. [13], as well as by Polycarpou and Komodromos [14]. The results of the investigations indicated that the response of the base-isolated buildings can be substantially modified due to structural pounding, as compared to the response of the structures with fixed bases. Masroor and Mosqueda [15] performed a series of earthquake simulator experiments to assess performance limit states of seismically isolated buildings under strong ground motions, confirming previous observations concerning the behaviour of base-isolated structures exposed to collisions during earthquakes. Naderpour et al. [16–18] investigated the results of different impact force formulas and compared them in terms of dissipated energy and suggested an equation to determine impact damping ratio. They showed numerically that the value of impact damping depends significantly on structural displacement, velocity and acceleration, as well as on the stiffness of impact spring, which is applied in the impact force model. Moreover, Miari et al. [19] analyzed different recommendations concerning appropriate gap size between structures to prevent pounding indicating on differences between them. Papadrakakis et al. [20] applied the Lagrange multiplier solution method to study the earthquake-induced collisions between adjacent buildings with different dynamic parameters and presented an effective method of testing the impacts between two, or more, buildings. A solution scheme was also suggested, and the correlation between numerical and analytical results was found to be satisfactory. Shakya and Wijeyewickrema [21] described the analysis of mid-column seismic pounding of reinforced concrete buildings of various heights, including the aspects of soil-structure interaction. The results of the study, concerning two configurations of buildings, indicated that the mid-column interactions can be more severe comparing the floor-to-floor pounding. Kajita et al. [22] performed collision tests and simulations, proving that the maximum impact force can be roughly estimated from the simulation analyses. Crozet et al. [23] carried out the detailed shaking table experimental tests, which can be utilized as reference tests to be compared with the results of numerical analyses. Moreover, an extensive analysis concerning collisions of buildings during earthquakes was presented in the doctoral dissertation by Isteita [24]. The research was mainly focused on the required separation distance to preclude pounding between neighbouring buildings, as well as on the risk of damage and the costs associated with it. Also, Isteita and Porter [25] conducted a study on the safe distance between buildings using a number of different methods for verification. Further studies on earthquake-induced collisions between insufficiently separated buildings, or bridge segments, were also recently conducted (see [26–32], for example).

In spite of the fact that structural pounding during seismic excitations has been much advanced, little attention has been paid to the analysis of peak impact forces expected as the result of collisions during the time of the earthquake. Meanwhile, information about the parameter might be very important to mitigate structural pounding during earthquakes, i.e., for the design of linking elements (see [33], for example). Therefore, the aim of the present paper was to show the results of the study focused on determination of peak impact forces during collisions between buildings exposed to different seismic excitations.

It should be underlined that there are many factors used to parameterize the effects of ground motions from the point of view of possible earthquake-induced structural damage (see [34,35]). These factors include the earthquake intensity, frequency contents, PGA value and duration of excitation. The frequency contents and PGA are often considered to be the most important parameters among them [34,36]. Therefore, the analysis described in the present paper was especially focused on the effects of these parameters on pounding-involved structural response under seismic excitation. The numerical investigation was conducted for ground motions characterized by various PGA values and frequency contents.

It should be added that the interpretation of the influence of the above parameters can be carried out using the probabilistic approach. Then, the essence of the investigation was to determine of the degree of uncertainty and probability (dependent, output variables) depending on the chosen factors (independent, input variables). The basic analysis of this type is the sensitivity analysis of the input parameters, which focused on checking how the resulting value (dependent) modified the response when the input values were changed. The Monte Carlo simulation (see [37–39]) and the first-order second-moment method can be used for such analysis [40]. In the stochastic structural analysis, the seismic response of a structure can be obtained using a random vibration method, in which ground motion is modelled as a random process [37,41,42]. Moreover, Yazdani and Eftekhari [37] noticed that for various magnitudes of earthquakes, the uncertainty of the ground motion variables is more significant than the uncertainty of structural properties. In [34], after conducting extensive study, Elassaly stated that low-frequency earthquakes are associated with relatively low PGA values, while high-frequency earthquakes would have relatively high PGA values. It was also proved that the reinforced concrete buildings subjected to earthquakes with the same PGA but with lower predominant frequencies would generally result in higher values of overall damage rates, as compared to other frequency content categories [34]. Therefore, the stochastic analysis was proposed to be conducted especially for bridges with large spans and for high buildings [37]. Consequently, in the case of these structures, the research should be focus on developing the analysis taking into account properties of ground motion using the stochastic approach.

## 2. Materials and Methods

The investigation was focused on the earthquake-induced structural pounding between two adjacent single-story buildings. In the analysis, the numerical model, in which both colliding structures were simulated as single-degree-of-freedom systems (see Figure 1), were used. The dynamic equation of motion for the case considered can be written as:

$$\begin{bmatrix} m_1 & 0 \\ 0 & m_2 \end{bmatrix}\begin{bmatrix} \ddot{x}_1(t) \\ \ddot{x}_2(t) \end{bmatrix}+\begin{bmatrix} C_1 & 0 \\ 0 & C_2 \end{bmatrix}\begin{bmatrix} \dot{x}_1(t) \\ \dot{x}_2(t) \end{bmatrix}+\begin{bmatrix} K_1 & 0 \\ 0 & K_2 \end{bmatrix}\begin{bmatrix} x_1(t) \\ x_2(t) \end{bmatrix}+\begin{bmatrix} F_{imp}(t) \\ -F_{imp}(t) \end{bmatrix}=-\begin{bmatrix} m_1 & 0 \\ 0 & m_2 \end{bmatrix}\begin{bmatrix} \ddot{x}_g(t) \\ \ddot{x}_g(t) \end{bmatrix} \quad (1)$$

where $x_i(t)$, $\dot{x}_i(t)$, $\ddot{x}_i(t)$, $C_i$ and $K_i$ are the horizontal displacement, velocity, acceleration, damping coefficient and stiffness coefficient for building $i$ ($i$ = 1, 2), respectively, $\ddot{x}_g(t)$ stands for the acceleration input ground motion and $F_{imp}(t)$ is the impact force, which is defined as [8]:

$$\begin{array}{lll} F_{imp}(t) = 0 & \text{for } \delta(t) \le 0 & \text{(no contact)} \\ F_{imp}(t) = \overline{\beta}\delta^{\frac{3}{2}}(t) + \overline{c}(t)\dot{\delta}_{ij}(t) & \text{for } \delta(t) > 0 \text{ and } \dot{\delta}(t) > 0 & \text{(contact } - \text{ approach period)} \\ F_{imp}(t) = \overline{\beta}\delta^{\frac{3}{2}}(t) & \text{for } \delta(t) > 0 \text{ and } \dot{\delta}(t) \le 0 & \text{(contact } - \text{ restitution period)} \end{array} \quad (2a)$$

$$\delta(t) = x_1(t) - x_2(t) - d;\ \overline{c}(t) = 2\overline{\xi}\sqrt{\overline{\beta}\sqrt{\delta(t)}\frac{m_1 m_2}{m_1 + m_2}} \quad (2b)$$

where $m_1$ and $m_2$ are masses of colliding buildings, $\overline{\beta}$ stands for the impact stiffness parameter which depends on material properties and geometry of the colliding structures, $d$ is the initial separation gap and $\overline{\xi}$ denotes the impact damping ratio which can be determined from the formula [36]:

$$\overline{\xi} = \frac{(1 - CR)}{CR^{(\alpha+0.204)} + 3.351CR\pi} CR^{0.204}; \ \alpha = 1.05CR^{0.653} \tag{3}$$

where $CR$ is the coefficient of restitution, which accounts for the energy dissipation during impact and depends on geometry and material of colliding surfaces, as well as on the value of relative prior-impact velocity between structures [8]. The value of $CR$ can be assessed experimentally by dropping a sphere on a massive plane plate of the same material from a height $h$ and observing the rebound height $h^*$. Then, the following formula was used [8]:

$$CR^2 = \frac{h^*}{h} \tag{4}$$

$CR = 1$ ($h^* = h$) means fully elastic collision and $CR$ approaching 0 ($h^* \sim 0$) deals with fully plastic impact.

Moreover:

$$T_i = 2\pi \sqrt{\frac{m_i}{K_i}}; \quad \xi_i = \frac{C_i}{2\sqrt{K_i m_i}} \tag{5}$$

where $T_i$, $\xi_i$ is the natural period and the structural damping ratio for building $i$ ($i = 1, 2$), respectively.

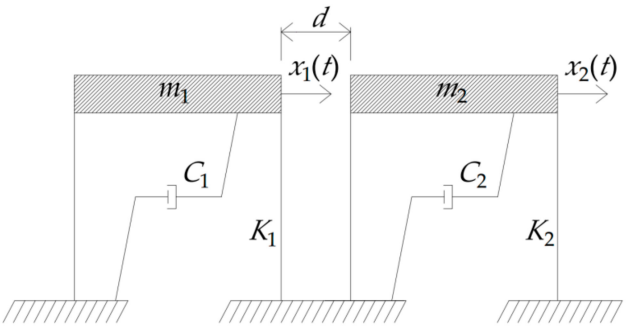


**Figure 1.** Model of interacting two adjacent single-storey buildings.

The numerical analysis was conducted for the following basic parameters: $T_1 = 0.25$ s, $T_2 = 0.65$ s, $m_1 = 1250$ kg, $m_2 = 3150$ kg, $\xi_1 = 0.05$, $\xi_2 = 0.05$, $d = 0.5$ cm and $CR = 0.65$. A time-stepping integration procedure with the constant time step of 0.0001 s was applied to solve the dynamic equation of motion (1). The numerical investigation was carried out for more than 50 different ground motions. Due to limitation of the space, the representative results, obtained for nine selected records (see Table 1 for general properties of ground motions and Figure 2 for their displacement and acceleration response spectra), are shown in this paper.

**Table 1.** Ground motion records used in the analysis.

| Earthquake | Date | Magnitude | Station | Component | PGA (cm/s$^2$) |
|---|---|---|---|---|---|
| Loma Prieta | 17.10.1989 | 6.9 | Corralitos | NS | 631.51 |
| Kobe | 17.01.1995 | 7.2 | JMA | NS | 817.82 |
| Parkfield | 28.06.1966 | 6.2 | Jennings (CGS) | NS | 462.00 |
| El Centro | 18.05.1940 | 6.9 | El Centro | NS | 307.00 |
| San Fernando | 09.02.1971 | 6.6 | Pacoima Dam | N16°W | 1202.62 |
| Duzce | 12.11.1999 | 7.2 | Izmit | NS | 754.23 |
| Kocaeli | 17.08.1999 | 7.6 | Izmit | NS | 695.24 |
| Landers | 28.06.1992 | 7.3 | Baker | NS | 853.00 |
| Tabas | 16.09.1978 | 7.4 | Tabas | NS | 784.81 |

PGA—Peak ground acceleration.

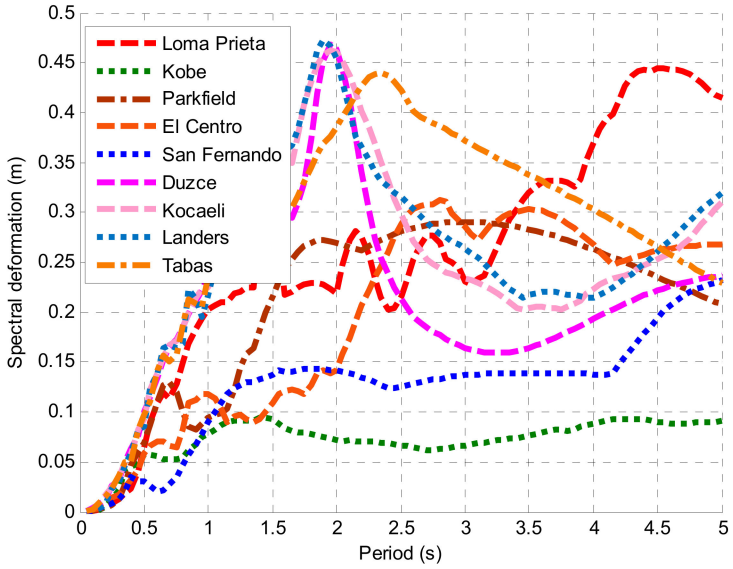


(**a**)

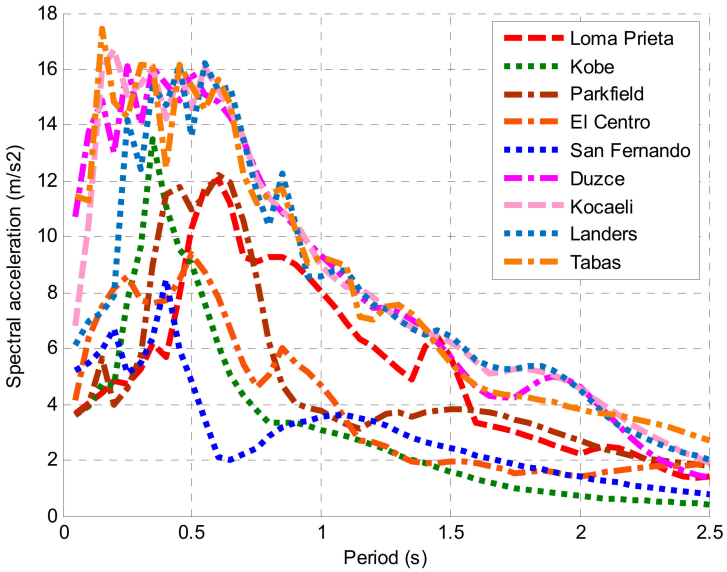


(**b**)

**Figure 2.** Displacement response spectra (**a**) and acceleration response spectra (**b**) of different earthquakes (structural damping: 0.05).

## 3. Results of the Analysis for Basic Parameters

The numerical investigation was carried out for the numerical model shown in Figure 1. First, the dynamic analysis was conducted for basic parameters of buildings exposed to different earthquakes. The representative examples of the results of the investigation, in the form of relation between impact force and impact displacement (penetration), are presented in Figure 3. The results shown in the figure indicate that the largest response was observed for the Duzce earthquake, for which the peak impact force and the peak impact displacement was as large as 7.6 kN and 10 cm, respectively. Meanwhile, the peak lateral design forces calculated for independently vibrating structures under this earthquake were equal to 20 kN and 44.4 kN for the left and the right building, respectively. Also, the response for the Kocaeli earthquake was found to be quite large, since the peak impact force was equal to 6.7 N and the peak impact displacement was equal to 9.3 cm. In the case of this ground motion, the peak lateral design forces calculated for independently vibrating structures were calculated as equal to 18.7 kN and 45.7 kN for the left and the right building, respectively. On the other hand, it can be seen from Figure 3 that the lowest response concerned the Loma Prieta earthquake, for which the peak impact force was equal to only 0.58 kN and the peak impact displacement did not exceed 2 cm. Meanwhile, the peak lateral design forces calculated for independently vibrating structures under this earthquake were equal to 5.9 kN and 34.6 kN for the left and the right building, respectively.

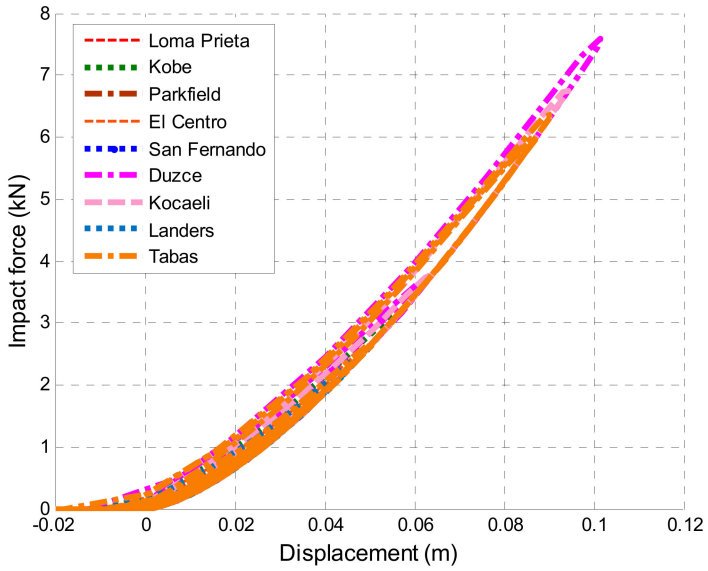


**Figure 3.** Impact forces with relation to impact displacement under different earthquakes.

## 4. Results of Parametric Study

In the second stage of numerical investigation, the parametric study was conducted for different structural natural periods, structural damping ratios, gap sizes between buildings and coefficients of restitution. When the effect of one parameter was investigated, the values of the others were kept unchanged. The representative examples of the results are shown below.

### *4.1. Effect of Structural Natural Period*

In order to evaluate the influence of the structural natural period on the pounding-involved response of buildings, the parameter for the left building was varied from 0 s to 1 s. The examples of the results in the form of the peak impact forces obtained for different values of the natural period of the left structure under different earthquakes are presented in Figure 4. Additionally, the largest values of peak impact forces are also summarized in Table 2. It can be seen from Figure 4 that the value of the peak impact force depended significantly on the structural natural period. Initially (in the range from 0 s to about 0.4 s), the peak impact forces increased slowly, and then the values grew

relatively rapidly, especially for the Tabas and Kocaeli earthquakes. The increase in the peak impact force with the structural natural period results from the fact that more flexible buildings exhibit larger displacements under earthquake excitations, as it can be clearly seen from the displacement response spectra shown in Figure 2a. In turn, larger displacements of structures substantially increase the probability of collisions during the time of ground motion. Moreover, the situation of two buildings approaching each other from different directions with high velocities is also often observed in the case of structures with larger natural periods, i.e., already for the structural period of 1 s.

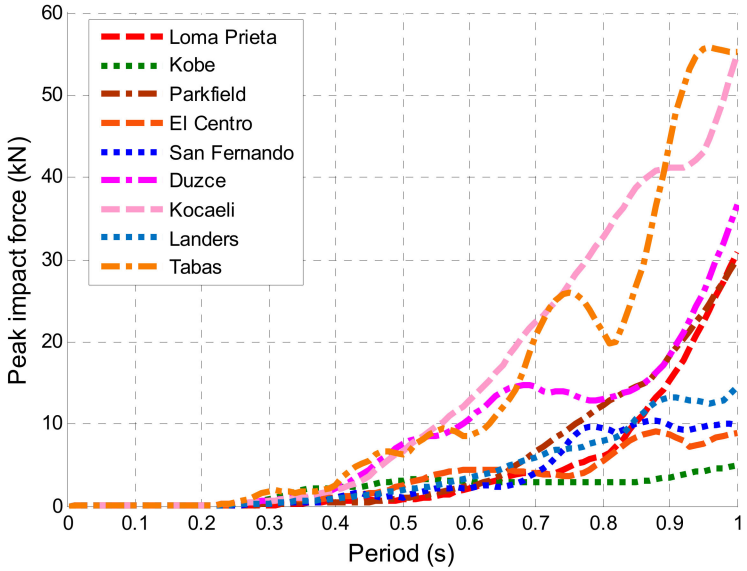


**Figure 4.** Peak impact force with relation to natural period of the left building under different earthquakes.

The peak lateral displacements with pounding and without pounding (independent vibrations of buildings) were also calculated in this stage of investigation for different periods of the left building under different seismic excitations. The results of the analysis are presented in Figure 5. The figure shows an increasing trend for the peak lateral displacement of the structure when the natural structural period increased, which is consistent with the results obtained for the peak impact force (see similarities between Figures 4 and 5). Moreover, by comparing Figure 5a with Figure 5b, it can be clearly seen that the influence of pounding on the behaviour of buildings can be substantial. It is, however, important to underline that collisions may either increase the peak displacement structural response or may also play a positive role, and the response can be reduced depending on the pounding scenario during the time of the earthquake (see also [8]). It can be seen from Figure 5 that, for the natural period of 1 s, as an example, the largest peak lateral displacements with and without pounding were equal to 38 cm and 41 cm, respectively, for the Tabas earthquake, while the minimum values were found to be equal to 7.8 cm and 9.0 cm, respectively, under the Kobe earthquake.

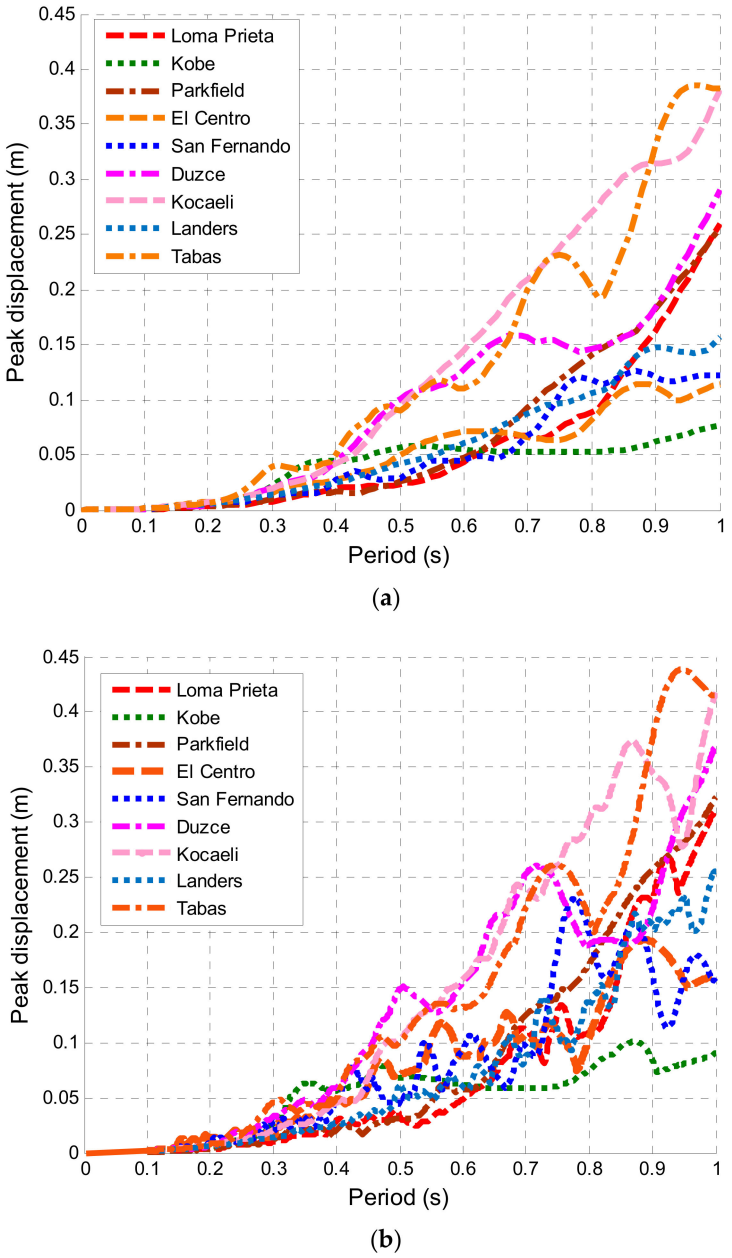


**Figure 5.** Peak lateral displacement with pounding (**a**) and without pounding (**b**) with relation to the natural period of the left building under different earthquakes.

In addition to the results shown in Figures 4 and 5, the values of the peak impact force with relation to spectral displacement (peak displacement of the left building without pounding) under different earthquakes are also presented in Figure 6. It can be seen form the figure that the plots for all ground motions followed a similar increase trend. Based on such results, a uniform simplified relationship can be derived, which can be used for the design purposes of closely spaced buildings exposed to different seismic excitations.

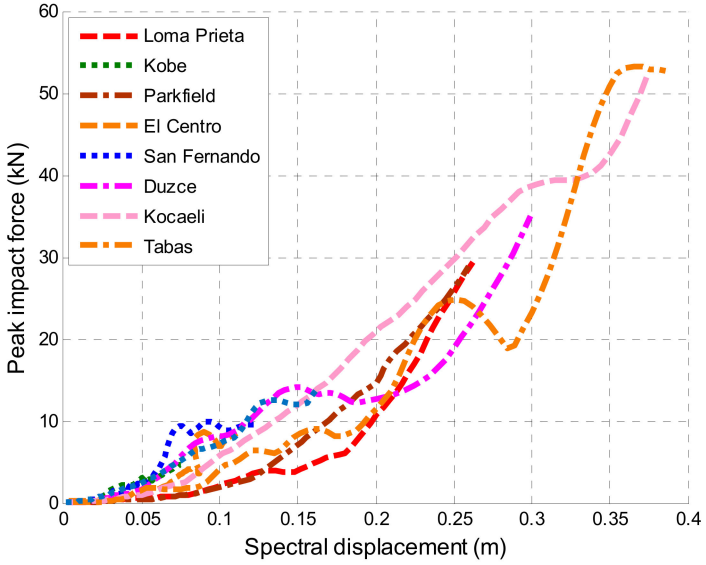


**Figure 6.** Peak impact force with relation to spectral displacement under different earthquakes.

**Table 2.** Largest peak impact forces—results for different structural periods.

| Earthquake | Largest Peak Impact Force (kN) |
|---|---|
| Loma Prieta | 30.0 |
| Kobe | 5.9 |
| Parkfield | 30.0 |
| El Centro | 9.3 |
| San Fernando | 9.9 |
| Duzce | 38.0 |
| Kocaeli | 57.0 |
| Landers | 12.0 |
| Tabas | 57.0 |

### *4.2. Effect of Structural Damping Ratio*

In the next stage of the parametric study, the influence of the structural damping ratio on the response of buildings was analysed. The range for the damping ratio (0.01–0.1) was defined to cover a wide range of possible values observed for real structures (see [43]). The results of the analysis for different values of damping ratio for both structures exposed to various earthquake excitations are shown in Figure 7. Additionally, the results for the typical value of the structural damping ratio of 0.05 are also summarized in Table 3. It can be clearly seen from Figure 7 that the peak impact force was considerably reduced when the structural damping ratio increased. The most noticeable reduction in the response was observed for the Duzce earthquake, for which the peak impact force was equal to 14 kN for the $\xi_1 = \xi_2 = 0.01$, and decreased to the value of 4.7 kN when $\xi_1 = \xi_2 = 0.1$. That represents the reduction by nearly 66%.

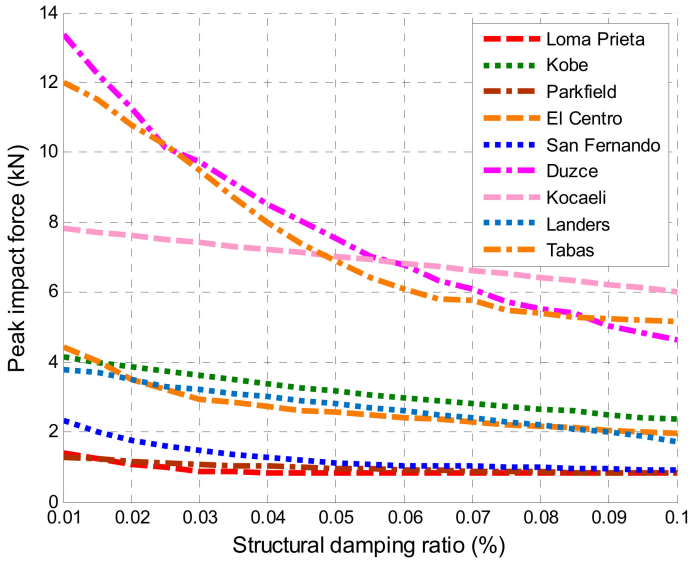


**Figure 7.** Peak impact force with relation to structural damping ratio under different earthquakes.

**Table 3.** Peak impact forces for the typical value of the structural damping ratio of 0.05.

| Earthquake | Peak Impact Force (kN) |
|---|---|
| Loma Prieta | 1.5 |
| Kobe | 3.6 |
| Parkfield | 1.5 |
| El Centro | 2.3 |
| San Fernando | 1.7 |
| Duzce | 7.8 |
| Kocaeli | 7.1 |
| Landers | 2.0 |
| Tabas | 6.2 |

### *4.3. Effect of Gap Size between Buildings*

In order to evaluate the influence of the in-between gap size on the response of buildings, the parameter was varied from 0 cm to 5 cm. The examples of the results in the form of the peak impact forces obtained for different gap size values under various earthquakes are presented in Figure 8. It can be seen from the figure that the peak impact force decreased as the gap size became larger until the separation distance was big enough to prevent pounding. This time, the largest decrease was observed for the Duzce, Tabas and Kocaeli earthquakes. The values of the largest peak impact forces (for the gap size equal to 0), as well as the minimum gap sizes between buildings preventing their pounding, are shown in Table 4. It should be mentioned that the obtained minimum in-between gap size values were lower than the spectral displacements at the period of a single structure. This effect resulted from the fact that the minimum in-between gap size preventing pounding was calculated based on the relative displacement between two adjacent buildings vibrating in a different way under seismic excitation. Therefore, it is possible that the left structure might considerably reduce the distance to the right one due to out-of-phase vibrations, and such a situation might take place only once during the whole time of the earthquake.

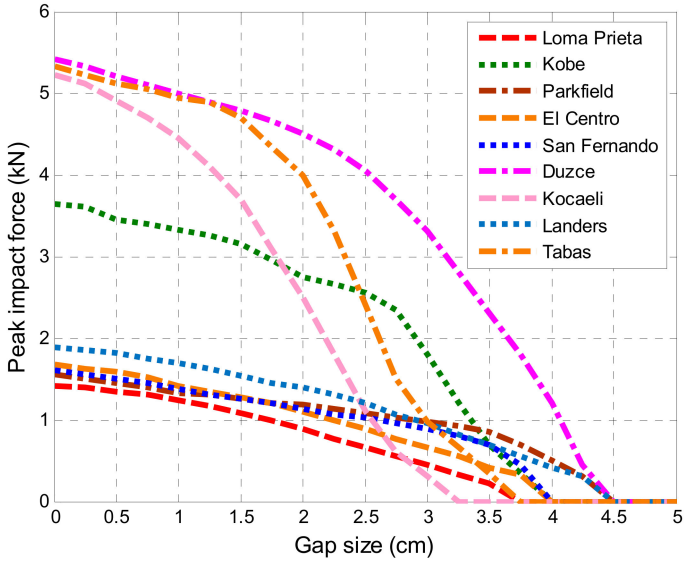


**Figure 8.** Peak impact force with relation to gap size between buildings under different earthquakes.

**Table 4.** Results for different gap sizes between buildings.

| Earthquake | Largest Peak Impact Force (kN) | Minimum Gap Size Preventing Pounding (cm) |
|---|---|---|
| Loma Prieta | 1.6 | 3.7 |
| Kobe | 3.8 | 4.0 |
| Parkfield | 1.6 | 4.5 |
| El Centro | 1.7 | 4.0 |
| San Fernando | 1.7 | 4.0 |
| Duzce | 5.7 | 4.5 |
| Kocaeli | 5.5 | 3.2 |
| Landers | 2.0 | 4.5 |
| Tabas | 5.6 | 3.7 |

### *4.4. Effect of Coefficient of Restitution*

In the final stage of the parametric study, the influence of the coefficient of restitution on the structural response was analysed. The results of the analysis for different values of the parameter ranging from 0 to 1 are shown in Figure 9. Additionally, the peak impact forces for *CR* approaching 0 and for the case when *CR* = 1 are shown in Table 5. It can be clearly seen from Figure 9 that the peak impact force decreased with the increase in the *CR* value, although this trend was not uniform. The significant decrease in the peak impact force value was observed for the range of *CR* between 0 and 0.1. Then, i.e., for *CR* larger than 0.1 and lower than 0.3, the decrease in the peak impact force value was much smaller. Finally, for *CR* larger than 0.3, the decrease in the peak impact force value was minimal. It can be seen in Table 5 that the overall decrease in the peak impact force was as large as 69% (San Fernando earthquake), 62% (Kobe earthquake), 59% (Parkfield and El Centro earthquakes), 57% (Tabas earthquake), 56% (Loma Prieta earthquake), 54% (Duzce earthquake), 50% (Kocaeli earthquake) and 26% (Landers earthquake).

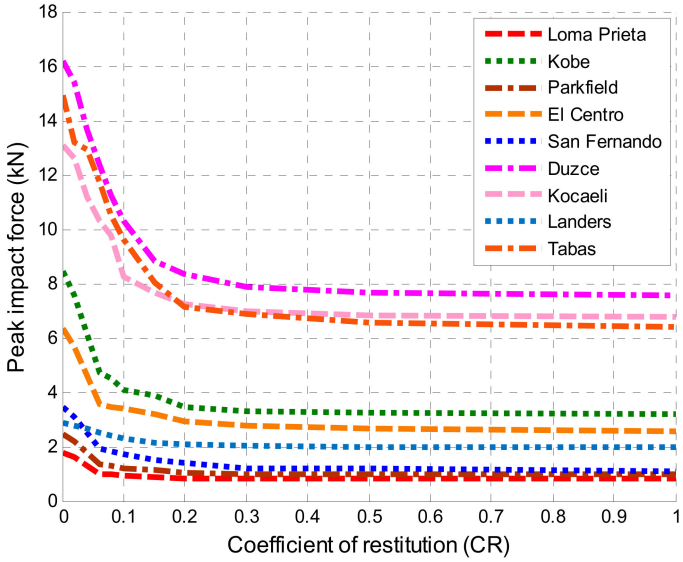


**Figure 9.** Peak impact force with relation to coefficient of restitution.

**Table 5.** Peak impact forces for two extreme values of coefficient of restitution.

| Earthquake | Peak Impact Force (kN) | |
|---|---|---|
| | $CR \sim 0$ | $CR = 1$ |
| Loma Prieta | 1.9 | 0.83 |
| Kobe | 8.4 | 3.2 |
| Parkfield | 2.5 | 1.0 |
| El Centro | 6.2 | 2.6 |
| San Fernando | 3.7 | 1.1 |
| Duzce | 16.0 | 7.5 |
| Kocaeli | 13.0 | 6.7 |
| Landers | 2.7 | 2.0 |
| Tabas | 15.0 | 6.4 |

## 5. Conclusions

The results of the study, which focused on the determination of peak impact forces during collisions between two buildings exposed to seismic excitations, are shown in the paper. A set of different ground motion records, with various PGA values and frequency contents, were considered in the study. First, pounding-involved numerical analysis was conducted for the basic parameters of colliding buildings. Then, the parametric study was carried out for different structural natural periods, structural damping ratios, gap sizes between buildings and coefficients of restitution.

The results of the analysis conducted for the basic structural parameters indicate that the largest response of the analyzed buildings was observed for the Duzce earthquake. The results of the parametric study show that the pounding-involved structural response depends substantially on all parameters considered in the analysis. In the case of the investigation conducted for different values of the structural natural period, the peak impact forces initially slowly increased, and then grew relatively rapidly, especially for the Tabas and Kocaeli earthquakes. The parametric study, which focused on the effect of the structural damping ratio, show that the peak impact force was considerably reduced when the structural damping ratio increased, with the most noticeable reduction in the response recorded for the Duzce earthquake. Also, the results for different values of the gap size between buildings show a similar trend. In the case of this parameter, the peak impact force considerably decreased as the gap size becomes larger until the separation distance was big enough to prevent pounding, and the largest decrease was observed for the Duzce, Tabas and Kocaeli earthquakes. Finally, the analysis conducted for different values of the coefficient of restitution indicate that the peak impact

force decreased nonuniformly with the increase in the *CR* value. In this case, the largest response was observed for the Duzce earthquake.

The results of the study presented in this paper clearly indicate that the value of the peak impact force expected during the time of ground motion does not really depend on the PGA value of the earthquake (see from Table 1 that the PGA values for the Duzce, Kocaeli and Tabas earthquakes are not very high with relation to other seismic excitations). On the contrary, considerable dependence of the peak impact force on the frequency contents of excitation (see Figure 2), as well as on the pounding scenario, was observed from the results of numerical simulations. It is therefore recommended that the peak impact force for buildings exposed to structural pounding during ground motions should be determined individually for the specific configuration of structures taking into account the design earthquake. However, it is important to underline that structures with substantially different natural periods are more vulnerable to collisions, since their relative velocity may change significantly during the time of the earthquake. It is also possible for them to approach each other from different directions with high velocities, which is the worst-case scenario. In such cases, large values of impact forces can be expected. Moreover, special attention should be paid to the effects of the frequency contents of the seismic excitation, as one of the most important parameters of the ground motion [34,37]. The investigation should be planned in such a way to be able to take into account the sensitivity analysis in order to determine the probability of the effects of frequency contents on possible earthquake-induced structural damage.

It should be added that connecting buildings by special link elements is one of the methods to mitigate earthquake-induced structural pounding. The approach concerns the application of stiff links, which allow the forces to be transmitted between structures, as well as some viscoelastic linking elements can be used to dissipate the energy during structural vibrations [33]. Other techniques might include the installation of rubber shock absorbers, polymer bumpers or collision shear walls, which can help in preventing sudden shocks due to collisions [44–47]. Another method to improve the behaviour of existing buildings preventing pounding is to increase their stiffness. The effect can be obtained by installation of additional bracing system or shear walls, which act as a part of the earthquake resistant system [48]. It is also possible to decrease the displacement response of buildings, and thus reduce the probability of earthquake-induced pounding, by increasing their damping properties. It can be obtained by providing supplemental energy dissipation devices, for example, in the form of diagonal elements connecting adjacent floor slabs [49].

A number of simplifications were introduced in the numerical model applied in the analysis described in the present paper. Therefore, further studies are needed to verify the influence of other effects which were not considered in the analysis. Future studies should especially focus on the influence of the nonlinear structural behaviour, which was outside the scope of the present paper. It can be expected that this effect might be important in the case of severe earthquakes, which may induce highly inelastic response of structures. In such cases, adopting a nonlinear numerical model (even a simplified bilinear hysteresis model) will allow us to obtain more accurate results.

**Author Contributions:** Methodology, S.M.K., H.N., R.C.B. and R.J.; Software, S.M.K.; Validation, S.M.K., H.N., R.C.B., A.J.-G. and R.J.; Formal analysis S.M.K.; Investigation, S.M.K., H.N., R.C.B. and R.J.; Writing—original draft, S.M.K.; Writing—review & editing, A.J.-G. and R.J. All authors have read and agreed to the published version of the manuscript.

**Funding:** This research received no external funding.

**Acknowledgments:** The authors would like to thank Seyed Mohammad Nazem Razavi for his help in conducting some numerical simulations.

**Conflicts of Interest:** The authors declare no conflict of interest.

## References


1. Anagnostopoulos, S.A. Pounding of building in series during earthquakes. *Earthq. Eng. Struct. Dyn.* **1988**, *16*, 443–456. [CrossRef]
2. Sołtysik, B.; Jankowski, R. Non-linear strain rate analysis of earthquake-induced pounding between steel buildings. *Int. J. Earth Sci. Eng.* **2013**, *6*, 429–433.
3. Chouw, N.; Hao, H. Study of SSI and non-uniform ground motion effect on pounding between bridge girders. *Soil Dyn. Earthq. Eng.* **2005**, *25*, 717–728. [CrossRef]
4. Jankowski, R. Pounding between superstructure segments in multi-supported elevated bridge with three-span continuous deck under 3D non-uniform earthquake excitation. *J. Earthq. Tsunami* **2015**, *9*, 1550012. [CrossRef]
5. Kasai, K.; Maison, B.F. Building pounding damage during the 1989 Loma Prieta earthquake. *Eng. Struct.* **1997**, *19*, 195–207. [CrossRef]
6. Northridge Earthquake of January 17, 1994—Reconnaissance Report. In *EERI Report 95–03*; Earthquake Engineering Research Institute: Oakland, CA, USA, 1995; Volume 1.
7. Anagnostopoulos, S.A. Equivalent viscous damping for modeling inelastic impacts in earthquake pounding problems. *Earthq. Eng. Struct. Dyn.* **2004**, *33*, 897–902. [CrossRef]
8. Jankowski, R. Non-linear viscoelastic modelling of earthquake-induced structural pounding. *Earthq. Eng. Struct. Dyn.* **2005**, *34*, 595–611. [CrossRef]
9. Jankowski, R. Analytical expression between the impact damping ratio and the coefficient of restitution in the non-linear viscoelastic model of structural pounding. *Earthq. Eng. Struct. Dyn.* **2006**, *35*, 517–524. [CrossRef]
10. Muthukumar, S.; DesRoches, R.A. Hertz contact model with nonlinear damping for pounding simulation. *Earthq. Eng. Struct. Dyn.* **2006**, *35*, 811–828. [CrossRef]
11. Ye, K.; Li, L.; Zhu, H. A note on the Hertz contact model with nonlinear damping for pounding simulation. *Earthq. Eng. Struct. Dyn.* **2008**, *38*, 1135–1142. [CrossRef]
12. Filiatrault, A.; Wagner, P.; Cherry, S. Analytical prediction of experimental building pounding. *Earthq. Eng. Struct. Dyn.* **1995**, *24*, 1131–1154. [CrossRef]
13. Komodromos, P.; Polycarpou, P.C.; Papaloizou, L.; Phocas, M.C. Response of seismically isolated buildings considering poundings. *Earthq. Eng. Struct. Dyn.* **2007**, *36*, 1605–1622. [CrossRef]
14. Polycarpou, P.C.; Komodromos, P. Earthquake-induced poundings of a seismically isolated building with adjacent structures. *Eng. Struct.* **2010**, *32*, 1937–1951. [CrossRef]
15. Masroor, A.; Mosqueda, G. Experimental simulation of base-isolated buildings pounding against moat wall and effects on superstructure response. *Earthq. Eng. Struct. Dyn.* **2012**, *41*, 2093–2109. [CrossRef]
16. Naderpour, H.; Barros, R.C.; Khatami, S.M.; Jankowski, R. Numerical study on pounding between two adjacent buildings under earthquake excitation. *Shock Vib.* **2016**, *2016*, 1504783. [CrossRef]
17. Naderpour, H.; Barros, R.C.; Khatami, S.M. Suggestion of an equation of motion to calculate damping ratio during earthquake based on cyclic procedure. *J. Theor. Appl. Mech.* **2016**, *54*, 963–973. [CrossRef]
18. Naderpour, H.; Khatami, S.M.; Barros, R.C. Prediction of critical distance between two MDOF systems subject to seismic excitation in terms of artificial neural networks. *Period. Polytech. Civ. Eng.* **2017**, *61*, 516–529.
19. Miari, M.; Choong, K.K.; Jankowski, R. Seismic pounding between adjacent buildings: Identification of parameters, soil interaction issues and mitigation measures. *Soil Dyn. Earthq. Eng.* **2019**, *121*, 135–150. [CrossRef]
20. Papadrakakis, M.; Mouzakis, H.; Plevris, N.; Bitzarakis, S. Lagrange multiplier solution method for pounding of buildings during earthquakes. *Earthq. Eng. Struct. Dyn.* **1991**, *20*, 981–998. [CrossRef]
21. Shakya, K.; Wijeyewickrema, A.C. Mid-column pounding of multi-story reinforced concrete buildings considering soil effects. *Adv. Struct. Eng.* **2019**, *12*, 71–85. [CrossRef]
22. Kajita, Y.; Kitahara, T.; Nishimoto, Y.; Otsuka, H. Estimation of maximum impact force on natural rubber during collision of two steel bars. In Proceedings of the First European Conference on Earthquake Engineering and Seismology, Geneva, Switzerland, 3–8 September 2006. Paper No. 488.
23. Crozet, V.; Politopoulos, I.; Chaudat, T. Shake table tests of structures subject to pounding. *Earthq. Eng. Struct. Dyn.* **2019**, *48*, 1156–1173. [CrossRef]
24. Isteita, M. Studies of Earthquake Pounding Risk and of Above-Code Seismic Design. Ph.D. Thesis, University of Colorado at Boulder, Boulder, CO, USA, 2019.

25. Isteita, M.; Porter, K. Safe distance between adjacent buildings to avoid pounding in earthquakes. In Proceedings of the 16th World Conference on Earthquake Engineering, Santiago, Chile, 8–13 January 2017. Paper No. 2532.
26. Elwardany, H.; Seleemah, A.; Jankowski, R. Seismic pounding behavior of multi-story buildings in series considering the effect of infill panels. *Eng. Struct.* **2017**, *144*, 139–150. [CrossRef]
27. Bamer, F.; Markert, B. A nonlinear visco-elastoplastic model for structural pounding. *Earthq. Eng. Struct. Dyn.* **2018**, *47*, 2490–2495.
28. Kun, C.; Yang, Z.; Chouw, N. Seismic response of skewed bridges including pounding effects. *Earthq. Struct.* **2018**, *14*, 467–476.
29. Maniatakis, C.A.; Spyrakos, C.C.; Kiriakopoulos, P.D.; Tsellos, K.P. Seismic response of a historic church considering pounding phenomena. *Bull. Earthq. Eng.* **2018**, *16*, 2913–2941. [CrossRef]
30. Fatahi, B.; Van Nguyen, Q.; Xu, R.; Sun, W.J. Three-dimensional response of neighboring buildings sitting on pile foundations to seismic pounding. *Int. J. Geomech.* **2018**, *18*, 04018007. [CrossRef]
31. Li, C.; Bi, K.; Hao, H. Seismic performances of precast segmental column under bidirectional earthquake motions: Shake table test and numerical evaluation. *Eng. Struct.* **2019**, *187*, 314–328. [CrossRef]
32. Raheem, S.E.A.; Fooly, M.Y.; Shafy, A.G.A.; Taha, A.M.; Abbas, Y.A.; Latif, M.M.A. Numerical simulation of potential seismic pounding among adjacent buildings in series. *Bull. Earthq. Eng.* **2019**, *17*, 439–471. [CrossRef]
33. Jankowski, R.; Mahmoud, S. Linking of adjacent three-storey buildings for mitigation of structural pounding during earthquakes. *Bull. Earthq. Eng.* **2016**, *14*, 3075–3097. [CrossRef]
34. Elassaly, M. Effects of ground motion characteristics on damage of RC buildings: A detailed investigation. *Int. J. Civ. Environ. Eng.* **2015**, *9*, 693–701.
35. Song, R.; Li, Y.; van de Lindt, J.W. Impact of earthquake ground motion characteristics on collapse risk of post-mainshock buildings considering aftershocks. *Eng. Struct.* **2014**, *81*, 349–361. [CrossRef]
36. Khatami, S.M.; Naderpour, H.; Barros, R.C.; Jakubczyk-Gałczyńska, A.; Jankowski, R. Effective formula for impact damping ratio for simulation of earthquake-induced structural pounding. *Geosciences* **2019**, *9*, 347. [CrossRef]
37. Yazdani, A.; Eftekhari, S.N. The effect of structural properties and ground motion variables on the global response of structural systems. *Civ. Eng. Environ. Syst.* **2015**, *32*, 216–229. [CrossRef]
38. Dolsek, M. Incremental dynamic analysis with consideration of modeling uncertainties. *Earthq. Eng. Struct. Dyn.* **2009**, *38*, 805–825. [CrossRef]
39. Jankowski, R.; Walukiewicz, H. Modeling of two-dimensional random fields. *Probabilistic Eng. Mech.* **1997**, *12*, 115–121. [CrossRef]
40. Baker, J.W.; Cornell, C.A. Uncertainty propagation in probabilistic seismic loss estimation. *Struct. Saf.* **2008**, *30*, 236–252. [CrossRef]
41. Boore, D.M. Simulation of ground motion using the stochastic method. *Pure Appl. Geophys.* **2003**, *160*, 635–676. [CrossRef]
42. Jankowski, R.; Wilde, K. A simple method of conditional random field simulation of ground motions for long structures. *Eng. Struct.* **2000**, *22*, 552–561. [CrossRef]
43. Chopra, A.K. *Dynamics of Structures: Theory and Applications to Earthquake Engineering*; Prentice Hall: Upper Saddle River, NJ, USA, 1995.
44. Polycarpou, P.C.; Komodromos, P.; Polycarpou, A.C. A nonlinear impact model for simulating the use of rubber shock absorbers for mitigating the effects of structural pounding during earthquakes. *Earthq. Eng. Struct. Dyn.* **2013**, *42*, 81–100. [CrossRef]
45. Sołtysik, B.; Falborski, T.; Jankowski, R. Preventing of earthquake-induced pounding between steel structures by using polymer elements—Experimental study. *Procedia Eng.* **2017**, *199*, 278–283. [CrossRef]
46. Falborski, T.; Jankowski, R.; Kwiecień, A. Experimental study on polymer mass used to repair damaged structures. *Key Eng. Mater.* **2012**, *488–489*, 347–350. [CrossRef]
47. Anagnostopoulos, S.A.; Karamaneas, C.E. Use of collision shear walls to minimize seismic separation and to protect adjacent buildings from collapse due to earthquake-induced pounding. *Earthq. Eng. Struct. Dyn.* **2008**, *37*, 1371–1388. [CrossRef]

48. Divyashree, M.; Bhavyashree, B.N.; Siddappa, G. Comparison of bracing and shear walls as seismic strengthening methods to buildings with plan irregularities. *Int. J. Res. Eng. Technol.* **2014**, *3*, 205–210.
49. Patel, C.C.; Jangid, R.S. Seismic response of dynamically similar adjacent structures connected with viscous dampers. *IES J. Part A Civ. Struct. Eng.* **2010**, *3*, 1–13. [CrossRef]